

The rate of type Ia Supernovae and the Star Formation History

L. Greggio and E. Cappellaro

INAF, Osservatorio Astronomico di Padova, Vicolo dell'Osservatorio 5,35127 Padova, Italy

Abstract. The scaling of the rate of type Ia Supernovae (SNIa) with the parent galaxies' color provides information on the distribution of the delay times (DTD) of the SNIa progenitors. We show that this information appears to depend on the photometric bands used to trace the stellar age distribution and mass-to-light ratio in the parent galaxies. Using both $U - V$ and $B - K$ colors to constrain the star formation history, we model the SNIa rate as a function of morphological galaxy type for different DTDs. The comparison with the observed rate per unit B and K band luminosity yields consistent results, although the large error bars allow us to exclude only very flat and very narrow DTDs. The number of SNIa events per unit mass from one stellar generation results of $\sim 0.002-0.003 M_{\odot}^{-1}$.

Keywords: supernovae, stellar evolution

PACS: 97.60.Bw;98.62.Lv

INTRODUCTION

While it is generally believed that the progenitors of type Ia Supernovae (SNIa) are close binary systems, the evolutionary path leading to the final explosion is still unclear. As a consequence, a variety of distributions of the delay time (i.e. the time between the birth of the binary and the SNIa event) is possible, according to different scenarios for SNIa progenitors. The distribution of the delay times (DTD) determines the rate of injection of energy and nucleosynthetic products from SNIa to the interstellar medium (ISM); therefore, it is a key ingredient for modelling the evolution of galaxies, as well as of the intracluster and intergalactic medium. The interplay of the DTD and Star Formation History (SFH) for determining the SNIa rates in stellar systems has been studied by several authors ([15],[11],[8]). For a stellar system born according to a SF rate (SFR) given by $\psi(t)$, the SNIa rate at epoch t is:

$$\dot{n}_{\text{Ia}}(t) = k_{\text{Ia}} \int_{t=0}^t \text{DTD}(t_{\text{d}}) \psi(t - t_{\text{d}}) dt_{\text{d}} = k_{\text{Ia}} \times M_{\text{SF}} \times \langle \text{DTD} \rangle_{\psi} \quad (1)$$

where t_{d} is the delay time, k_{Ia} is the number of SNIa per unit mass in stars from one stellar generation, and M_{SF} is the total mass transformed into stars in the system up to the current epoch t . Therefore the time evolution of the SNIa rate, and/or the current rate in systems with different SFHs, can be used to constrain the shape of the DTD. At present, the cosmic evolution does not seem promising in this respect, due to i) the smearing effect of the cosmic SFH, which results into a wide age distribution in systems at intermediate and low redshift; ii) the large error bars affecting the determination of the rate at the highest redshifts ([6], [1], [2]). An alternative venue comes from the

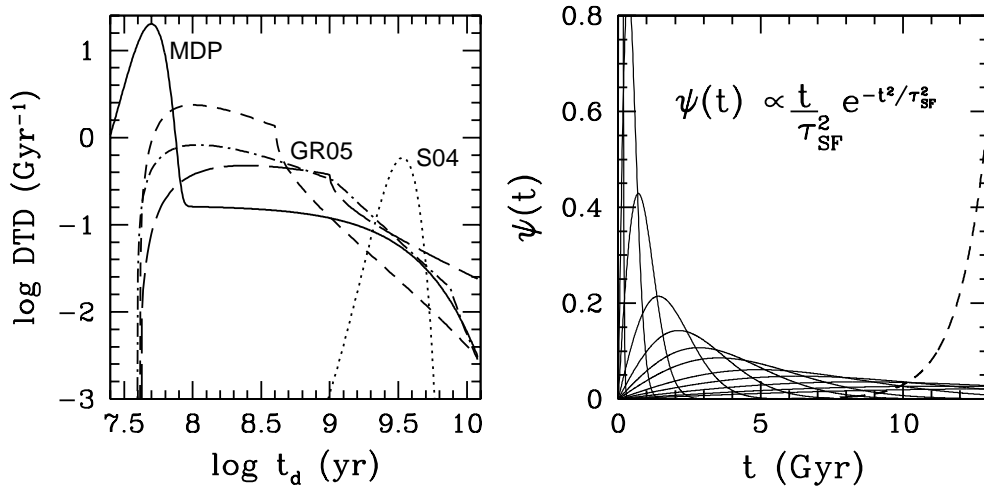


FIGURE 1. DTDs and SFRs used in this paper. Left: the MDP curve is constructed following the prescriptions in [11]; the S04 curve is a gaussian centered on $t_d = 3.4$ Gyr and with a width $\sigma = 0.68$ Gyr. The GR05 curves include a steep DD CLOSE (short dashed, $\beta_g = -0.975$, $\tau_{n,x} = 0.4$ Gyr), an SD model with a flat distribution of the mass ratios and a Salpeter distribution of the primaries' masses (dot-dashed), and a flat DD WIDE (long dashed, $\beta_a = 0$, $\tau_{n,x} = 1$ Gyr) models. See GR05 for the definition of the parameters. Right: SFRs generated by the labelled expression with τ_{SF} varying between 0.1 and 20 Gyr (solid); exponentially increasing SFR with e-folding time of 1 Gyr, started 10 Gyr ago (dashed).

analysis of the SNIa rate in different galaxies: the dependence of the rate from the age distribution of the parent stellar population is sensitive to the shape of the DTD; in turn, the age distribution can be traced using the colors of the stellar populations, so that the quantitative variation of the specific SNIa rate with the color of the parent galaxies constrains the DTD. This is investigated in this paper, through modelling and comparison with the observations.

DTDS AND STAR FORMATION HISTORIES

A variety of DTDs have been proposed in the literature, some empirical, others derived from stellar evolution theory. Fig. 1 shows the selection of functions considered here. The MDP ([11]) distribution accommodates two channels, one *prompt* and one *delayed*: the first includes events with delay times shorter than 0.1 Gyr; the second populates the remaining, very wide range of delay times up to one Hubble time, with a flat distribution between 0.1 and 3 Gyr, plus a progressive (rapid) depletion of events at longer delays. The time span and strength of the *prompt* channel are constrained by the controversial evidence of an enhanced SNIa rate in radio loud ellipticals. The S04 ([14]) distribution allows for a narrow range of delay times: this DTD appeared to provide the best fit of the evolution of the cosmic SNIa rate with redshift in combination with the cosmic SFR by [5]. The interpretation of the data which leads to these DTDs has been recently

questioned by [9]. The GR05 ([8]) models are rooted on stellar evolution, and are meant to describe a general shape for the DTD which follows from the characteristics of the clock of the explosion, and the distribution of the binary parameters in the progenitors' systems. In the Single Degenerate (SD) model a SNIa occurs when a White Dwarf (WD) accreting from an evolved companion reaches the Chandrasekhar mass; the Double Degenerate (DD) model corresponds to close binary WDs progenitors with total mass exceeding the Chandrasekhar limit, which merge due to gravitational waves radiation losses. The WIDE and CLOSE variety differ for the efficiency with which the first common envelope phase shrinks the orbit of the progenitors: this efficiency is higher in the CLOSE than in the WIDE case, leading to binary WDs with smaller separations, and then to a DTD characterized by a higher fraction of short delay times. The minimum mass of the secondary in the progenitor system, and the distribution of the separations of the DD systems at birth concur to shape the DTD for the DDs: here we choose two extreme cases, i.e. a steep DD CLOSE, and a flat DD WIDE model.

All the GR05 models encompass a wide range of delay times, reflecting either the evolutionary lifetimes of secondaries from 8 down to $0.8 M_{\odot}$ (SD models), or the wide range of gravitational wave radiation delays ensuing from a range of separations of the DD systems. At the same time, all the models are more populated at short, rather than long delays, basically due to the higher evolutionary rate off the main sequence of massive stars, compared to low mass stars. The late epoch drop of the DTD for the SD model is caused by the requirement of making up the Chandrasekhar mass in systems with progressively less massive secondaries. The smooth shapes of the GR05 DTDs reflect the assumption of continuous distributions of the binary parameters in SNIa progenitors, between wide limits. Conversely, the S04 DTD requires a very narrow range of these parameters. Compared to the MDP function, the GR05 models lack very early events. The minimum delay time for the latter models is fixed by the evolutionary lifetime of the most massive secondary in the progenitor systems, which is not well constrained. A maximum mass of 8 (10) M_{\odot} implies a minimum delay time of $\simeq 36(25)$ Myr, if core overshooting occurs during evolution; or $\simeq 32$ Myr for a standard (no overshoot) $8 M_{\odot}$ track. The GR05 models adopt a minimum delay time of 40 Myr, but a shorter delay could be applicable. The main difference between the MDP and the GR05 DTDs is the sharp drop in the former at a delay time of 0.1 Gyr, which corresponds to an evolutionary mass of $\simeq 5 M_{\odot}$. In the GR05 models nothing special happens when the secondary mass drops below $5 M_{\odot}$, as the distribution of the binary parameters (in SNIa progenitor systems) is assumed to be continuous across this mass.

The MDP and GR05 DTDs imply that the younger the stellar system, the higher its SNIa rate per unit mass, since these DTDs favour early, rather than late, events. The S04 DTD, instead, predicts a maximum rate in systems with a high fraction of intermediate age stars. To proceed with a quantitative fit of the specific SNIa rate as a function of the parent galaxy properties we need to specify the age distribution of stars in galaxies. Following [7] we consider the family of SFRs illustrated as solid lines in the right panel of Fig. 1. We assumed that all galaxies started to form stars 13 Gyr ago and are currently active, but, going from early to late type galaxies, the peak of the SF activity moves to younger ages, and the age distribution becomes wider. The results of the convolution of the DTDs with this family of SFH is presented in the next section. A SFH skewed towards the current epoch is also considered, to reproduce the colors of the

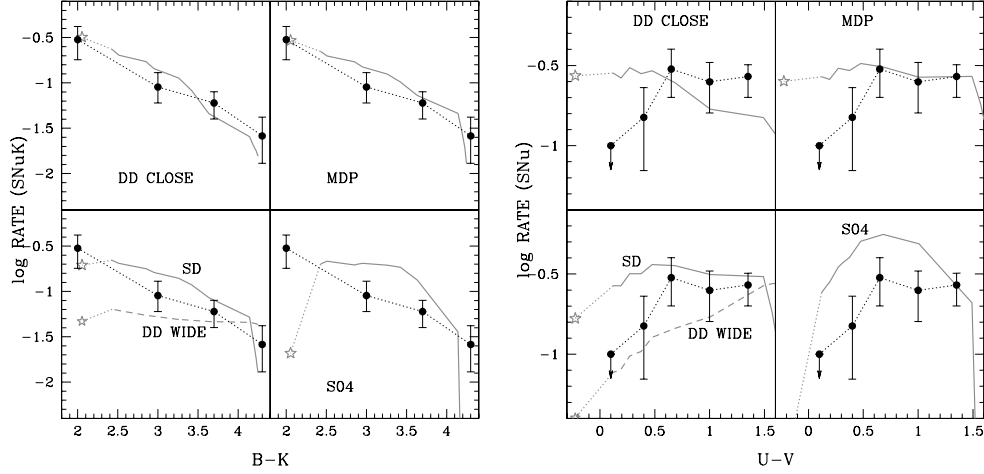


FIGURE 2. SNIa rates as function of the parent galaxy colors per unit K -band (left) and B -band (right) luminosity. Observational determinations are plotted as filled dots together with their error bars. The grey lines are models obtained with the DTDs (as labelled) and SFRs in Fig. 1. The star shows the prediction of the exponentially increasing SFR. The models assume a SNIa productivity $k_{\text{Ia}} = 0.001$ and $0.003 M_{\odot}^{-1}$ for the DD WIDE and all others models, respectively. The metallicity is assumed to correlate with τ_{SF} ; specifically: $Z=0.02$ for $\tau_{\text{SF}} \leq 3\text{Gyr}$; $Z=0.008$ for $3\text{Gyr} < \tau_{\text{SF}} \leq 6\text{Gyr}$; $Z=0.004$ for $6\text{Gyr} < \tau_{\text{SF}} \leq 9\text{Gyr}$; $Z=0.001$ for $\tau_{\text{SF}} > 9\text{Gyr}$ and for the exponentially increasing SFR.

bluest galaxies (in $B - K$).

FITTING THE OBSERVED SNIa RATES IN NEARBY GALAXIES

The full dots in Fig. 2 show the SNIa rate per unit luminosity as a function of the color of the parent galaxy from [10] (left panel) and from [4] (right panel). Rather than considering the SNIa rate per unit stellar mass, as done in [11], we prefer to fit the rate per unit luminosity which is a fully observational quantity, whereas the rate per unit mass rests upon a relation between the mass-to-light ratio and the galaxy color based on stellar population models. It can be noticed that, while the rate per unit K band luminosity is much larger in blue (young) galaxies than in red (old) ones, the rate per unit B band luminosity is lower in the bluest objects, and it is virtually constant in galaxies with $U - V \geq 0.5$. It is generally believed that L_K traces mass better than L_B : the data in the left panel of Fig. 2 would imply that, going from old to young stellar systems, the rate per unit mass increases, as predicted by the MDP and GR05 DTDs. At the same time, the L_B/M ratio is larger in young systems, so that the trend of the rate in SNU's depends on whether L_B/M increases faster than the rate per unit mass as the average age of the stellar population becomes younger. The data in the right panel in Fig. 2 seem to indicate that at $U - V > 0.5$ the two factors scale in the same way, while in the bluest galaxies the increase of the L_B/M ratio is the dominating effect. The grey lines in Fig. 2 show the theoretical relations as given by Eq. (1) for the DTDs and SFHs plotted on Fig. 1. The colors of the model galaxies result from population synthesis computations based

on simple stellar populations (SSP) models by [13]. A trend of decreasing metallicity with increasing τ_{SF} has been adopted to construct the galaxy colors. In spite of the low metallicity, the $B - K$ color of the model with $\tau_{\text{SF}}=20$ Gyr is redder than the bluest bin of data in [10]. This color can be reproduced by assuming a SFR strongly peaked at the current epoch: the star indicates the model predictions obtained with the exponentially increasing SFR shown in Fig. 1. Similar to previous conclusions (e.g. [11], [8]), the comparison between models and observations of the rate in SNUK indicates that the DTD needs to be mostly populated at the short delay times: the DD WIDE model predicts a flat specific rate with the parent galaxy color, and the S04 DTD implies a maximum rate in galaxies with intermediate average age, hence intermediate colors. None of the models, however, seems able to fit the trend of the rate in SNU's with the parent galaxy $U - V$ color. The increase of the rate per unit mass from intermediate age to young galaxies predicted by the DD CLOSE and the MDP curves matches the increase of the L_{B}/M ratio, so that the latest galaxy types should have about the same SNIa rate in SNU's as spiral galaxies. For the other DTDs we do obtain a lower rate in the bluest galaxies, but the overall trend of the data is not well reproduced. Notice that on Fig. 2 we compare only the shape of the relation between the SNIa rate and the parent galaxy color: a vertical shift of the models is allowed, given that the productivity k_{Ia} is a free parameter. Nevertheless, the same DTD does not fit the trend of the SNIa rate with the parent galaxy color on both observational planes. This conflict could be originated by several causes, including inadequacies in the adopted SFH laws and/or in the population synthesis models. In addition, although the global galaxy sample is the same, the observational relations in the two panels are not constructed for the same individual galaxies, as will be illustrated later. Computation of models with a broad family of SFHs, which include exponential and power law distributions, and with formation epochs varying between 3 and 13 Gyr ago lead to results very similar to those shown in Fig. 2. This does not exclude that some ad hoc variation of the SFH across the galaxy sample may lead to a unique indication on the DTD, but we clearly need to better constrain the age distribution of the stars in the various galaxy types which are used to build the observational relation. This is attempted next.

The galaxy sample from [4] includes 9346 galaxies from the RC3 catalogue, which provides B magnitudes for all of them, morphological type T for most (actually 9279 galaxies), and $U - B$, $B - V$ only for a subset. The $U - V$ color can be computed only for 1796 galaxies of the sample, which may be a small number to derive a robust relation between the SNIa rate with the properties of the parent galaxy. Cross correlating this galaxy sample with 2MASS yields infrared magnitudes for 6562 objects, for all of which the $B - K$ color can be computed. Although this is a large sample, the maximum exploitation of the data base is realized by examining the SNIa rate as a function of the parent galaxy morphological type. To do that we need to relate T to the SFH in the different galaxies. The model colors computed for the family of SFHs in Fig. 1 and different values of the metallicity (fixed metallicity for each SFH) are shown as black lines in the left diagram of Fig. 3, superimposed on the colors of the 1108 galaxies of the sample for which both $U - V$ and $B - K$ are available. These models encompass most of the data, and fairly describe the average trend of both colors becoming progressively redder with the star formation timescale becoming shorter. It also seems that the later galaxy types require lower metallicity compared to the earlier types, which is reasonable,

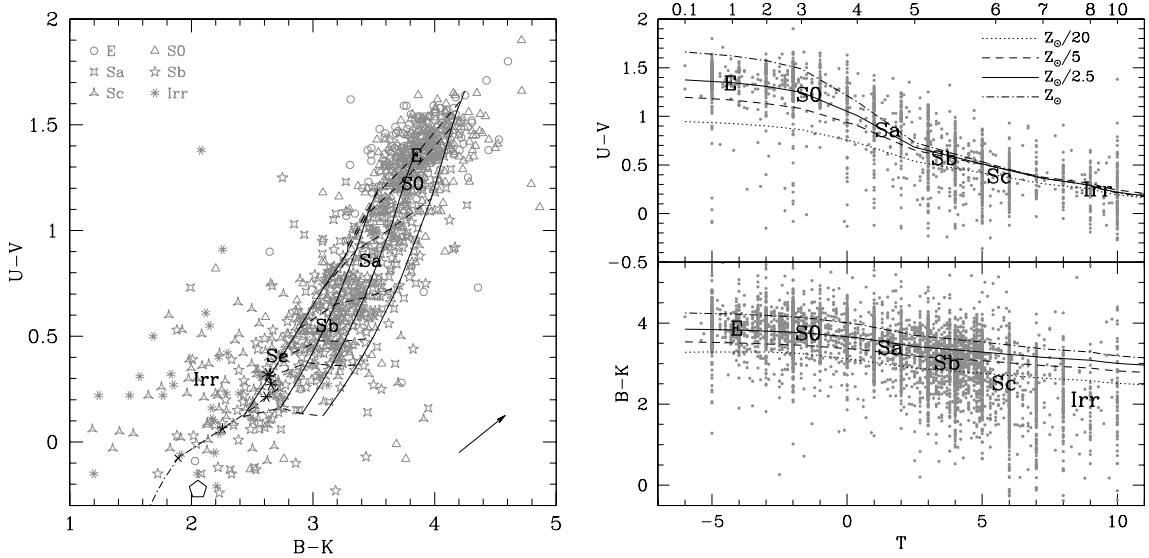


FIGURE 3. Calibration of the parameter τ_{SF} versus galaxy type T . Left: two color diagram for the galaxies (no reddening correction applied); the symbols encode the galaxy type, as labelled, and the letters are located at the average colors of the respective galaxy type. The solid lines show models with τ_{SF} increasing from 0.1 to 20 Gyr and a fixed metallicity of $Z = 0.001, 0.004, 0.008, 0.02$ (from left to right). The dashed lines connect models of different metallicity and fixed $\tau_{SF} = (1, 3, 4, 5, 6, 7, 20)$ Gyr (from top to bottom). The big pentagon shows the colors of a model with an exponentially increasing SFR (e-folding time of 1 Gyr), and metallicity $Z=0.001$. The arrow shows the reddening vector. The dot dashed line illustrates the effect of a recent burst of star formation, involving 10% of the total mass, superimposed on a young galaxy model (both components with $Z=0.001$); the dots show the colors for a burst age of (0.1, 0.15, 0.3, 0.5, 1) Gyr. Right: the colors are plotted as function of T for individual galaxies; the letters are located at the average color and T of the respective galaxy type. Lines show models as function of τ_{SF} (labelled on the top x-axis) for various metallicities, as labelled.

given the low metallicity in the interstellar medium of the latest galaxy types. However, there's a substantial number of galaxies which appear too blue in $B - K$ for their $U - V$ with respect to the models, especially among the latest types, for which even the average colors fall outside the models grid. We have checked a few possibilities to account for the location of the Irregular galaxies on this plot, including the effect of reddening, of different SSP models (e.g. [12]), of recent bursts of SF. None of these options leads to a fair fit of the colors of these galaxies. In particular, the colors of a recent burst are blue in both $B - K$ and $U - V$, as shown by the model with the exponential SFR, so that the addition of a recent burst does not populate the region occupied by the Irregulars. Notwithstanding this problem, we proceed with the calibration of the τ_{SF} parameter versus T by comparing the average colors of the various galaxy types with the models. This yields the correspondence shown in the right diagram on Fig. 3, which is very similar to what found by [7] from the comparison of the whole (average) spectral energy distributions of galaxies in the Virgo cluster with models based on this same SFHs and SSP models by [3]. The right diagram on Fig. 3 shows that this calibration is suitable for all galaxies with $U - V$ color (1796), and acceptable for all galaxies with $B - K$ color (6562), in the sample of [4]. The data show a sizeable scatter with respect to the models,

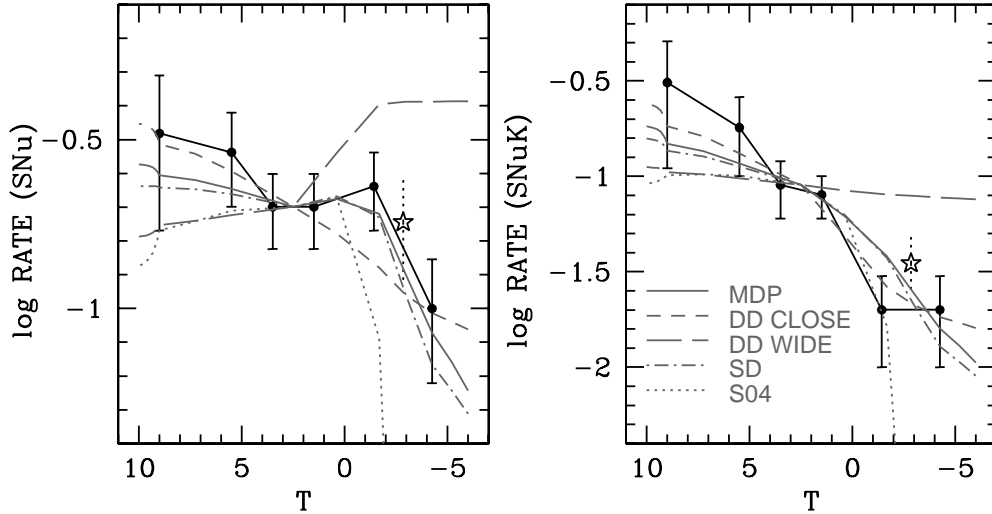


FIGURE 4. SNIa rates as function of the galaxy morphological type. Black points show the observational determinations; the star is the rate determined by combining the data for the E and S0 in one single class. Grey lines show the models shifted to reproduce the observed rate in Sb galaxies

especially for late type galaxies, but the average colors do lie on the theoretical lines, with the exception of the Irregulars, which again appear too blue in $B - K$ even for the lowest metallicity models.

Fig. 4 shows the SNIa rates as function of the morphological type compared to the predictions from Eq. (1) with the 5 selected DTDs, having adopted the τ_{SF} vs T calibration described above. The observed rates have been re-determined with respect to previous work, to incorporate the same partition of galaxy types as used in the calibration. In particular, the early type class (E+S0), whose rate is shown as a star, has been split into two separate classes. Within the large error bars, the two diagrams now yield the same conclusion with respect to the DTDs: the S04 function is ruled out because it highly under-predicts events in Es and S0s; the DD WIDE function is also ruled out because it over-predicts events in such galaxies; all other DTDs are instead compatible with the data. We notice that if the drop of the SNIa rate per unit B band luminosity going from S0 to Es is real, the MDP and SD models are favoured, since the DD models are featureless at long delay times. This drop is not appreciable when E and S0 galaxies are combined in one class.

The models in Fig. 4 have been shifted to reproduce the observed rate in Sb galaxies; the shift yields a value for the productivity k_{Ia} . For a Salpeter initial mass function, flattened below $0.5 M_{\odot}$, the productivity turns out $k_{Ia} \simeq (3, 1.5, 2, 2.3, 1.3) \cdot 10^{-3} M_{\odot}^{-1}$ respectively for the DD CLOSE, DD WIDE, SD, MDP and S04 models, with little variation when considering the rates in SNU's or in SNUK's. This same IMF has $\sim 0.06 M_{\odot}^{-1}$ stars with mass between 2 and $8 M_{\odot}$. Therefore, globally, it suffices that $\sim 4\%$ of these stars end their lives as SNIa. The MDP DTD requires that $\sim 50\%$ of the events originate from short lived progenitors, with masses larger than $\sim 5 M_{\odot}$. One stellar

generation provides $\sim 0.01 M_{\odot}^{-1}$ stars with mass between 5 and $8 M_{\odot}$. If 50% of the events in the calibrating Sb galaxies are produced by the *prompt* channel, its efficiency of SNIa production should be $\sim 0.5 \cdot 0.23 \simeq 0.12$, i.e. larger than in the other cases, but still acceptable.

CONCLUSIONS

The indications on the DTD from the fit of the specific SNIa rate as function of the parent galaxy colour appear inconsistent when considering different colors to trace the SFH and the M/L ratio. To overcome this problem, the age distribution of galaxies in the sample of [4] has been constrained on the two color plot which accounts for both $U - V$ and $B - K$ colors. In this way, it is possible to derive a calibration of the morphological type in terms of SFH, and proceed with fitting the trend of the specific SNIa rate as function of the morphological type. On this plane, the specific rates measured in SNu's and in SNuK's provide the same indication for the DTD, as well as similar values for the SNIa productivity from one stellar generation ($\sim 0.002 - 0.003 M_{\odot}^{-1}$). The constraints on the DTD are rather broad: the S04 distribution and a very flat DD WIDE model are ruled out, but all other models are acceptable. We notice that the parameters for the DD models have been intentionally chosen so as to maximize the difference between DD CLOSE and DD WIDE cases, and we anticipate that flatter DD CLOSE and steeper DD WIDE models are also acceptable. Our modelling does not reproduce the average $B - K$ of Irregular galaxies; however our conclusions on the DTD do not rely on the rate measured in these galaxies, but rather on the trend of the SNIa rate in the other morphological types. Stronger constraints on the age distributions in the various galaxies in the sample (e.g. from the analysis of their full spectral energy distributions), especially for the latest galaxy types, will enable us to derive stronger constraints on the DTD. In addition, a robust measurement of the rate in E and S0s separately will be very important to verify whether the DTD features a sizable drop at the long delays.

REFERENCES

1. G. Blanc, and L. Greggio, *NewAR* **13**, 606-618 (2008).
2. M. T. Botticella, et al., *A&A* **479**, 49 (2008).
3. G. Bruzual, and S. Charlot, *ApJ* **405**, 538-553 (1993).
4. E. Cappellaro, R. Evans, and M. Turatto, *A&A* **351**, 459 (1999).
5. M. Giavalisco, et al., *ApJ* **600**, L103-L106 (2004).
6. F. Foerster, et. al., *MNRAS* **368**, 1893-1904 (2006).
7. G. Gavazzi, et. al., *ApJ* **576**, 135-151 (2002).
8. L. Greggio, *A&A* **441**, 1055-1078 (2005).
9. L. Greggio, A. Renzini, and E. Daddi, *MNRAS* **388**, 829-837 (2008).
10. F. Mannucci, et al., *A&A* **433**, 807-814 (2005).
11. F. Mannucci, M. Della Valle, and N. Panagia, *MNRAS* **370**, 773-783 (2006).
12. C. Maraston, *MNRAS* **362**, 799-825 (2005).
13. P. Marigo, et al., *A&A* **482**, 883-905 (2008).
14. L.G. Strolger et al., *ApJ* **613**, 200-223 (2004).
15. P. Ruiz-Lapuente, A. Burkert, and R. Canal. *ApJ* **447**, L69-L72 (1995).